

Research Article

An Energy Conserving Numerical Scheme for the Dynamics of Hyperelastic Rods

Thorsten Fütterer,¹ Axel Klar,² and Raimund Wegener¹

¹ Fraunhofer Institut für Techno- und Wirtschaftsmathematik, Fraunhofer-Platz 1,
67663 Kaiserslautern, Germany

² Fachbereich Mathematik, Technische Universität Kaiserslautern, 67653 Kaiserslautern, Germany

Correspondence should be addressed to Axel Klar, klar@mathematik.uni-kl.de

Received 12 January 2012; Revised 21 June 2012; Accepted 5 July 2012

Academic Editor: Mapundi Banda

Copyright © 2012 Thorsten Fütterer et al. This is an open access article distributed under the Creative Commons Attribution License, which permits unrestricted use, distribution, and reproduction in any medium, provided the original work is properly cited.

A numerical method for special Cosserat rods based on Antman's description Antman, 2005 is developed for hyperelastic materials and potential forces. This method preserves the relevant properties of the underlying PDE system, namely, the orthonormality of the directors and the conservation of the energy.

1. Introduction

Elastic rods are considered in many fields of science and technology; see, for example, [1–3]. For the simulation of their dynamics, the correct description of the local and global physical properties and reasonable computation times are the essential requirements.

Over the past years many different approaches to the numerical simulation of elastic rods have been developed; see, for example, [4–9] for different approaches involving finite element methods, finite difference methods and discrete mechanics.

In this paper we use the description of the rod as a special one-dimensional Cosserat continuum following the formulation in Antman [10]. This is a geometrically correct one-dimensional description based on partial differential equations. This type of modeling fulfills the above requirements with respect to simplicity and correctness. Numerical schemes for the special case of Kirchhoff equations have been developed by Pai [1] (stationary) and Weber et al. [3] (instationary). Energy conservation and the directors' orthonormality are not strictly fulfilled in these schemes. Schemes for structural mechanics problems conserving energy and further invariants of the equation are developed, investigated, and applied, for example, in [11–13].

We formulate the kinematic and dynamic equations of the Cosserat rod theory in the so-called director-basis. The rod's curve $\bar{\mathbf{r}}$ and the outer potential force $\bar{\mathbf{f}}$ are the only fields described in an external Cartesian basis. For technical reasons we use a representation of the rotational group by unit-quaternions. We note that the first use of quaternions in geometrically-exact rod models was in [14], see also [15]. In Section 2 we present an overview of the model resulting in the following system:

$$\begin{aligned}\partial_t \bar{\mathbf{r}} &= D^{-1}(\mathbf{q}) \cdot \mathbf{p}, \\ \partial_t \mathbf{q} &= \mathbf{\Omega}(\mathbf{w}) \cdot \mathbf{q}, \\ \partial_t \mathbf{v} &= \partial_s \mathbf{p} + \mathbf{u} \times \mathbf{p} + \mathbf{v} \times \mathbf{w}, \\ \partial_t \mathbf{u} &= \partial_s \mathbf{w} + \mathbf{u} \times \mathbf{w}, \\ \partial_t \mathbf{p} &= \frac{1}{(\rho A)} \partial_s \mathbf{n} + \frac{1}{(\rho A)} \mathbf{u} \times \mathbf{n} + \mathbf{p} \times \mathbf{w} + \frac{1}{(\rho A)} D(\mathbf{q}) \cdot \bar{\mathbf{f}}, \\ \partial_t \mathbf{w} &= (\rho J)^{-1} \cdot \partial_s \mathbf{m} + (\rho J)^{-1} \cdot (\mathbf{u} \times \mathbf{m} + \mathbf{v} \times \mathbf{n} + ((\rho J) \cdot \mathbf{w}) \times \mathbf{w}).\end{aligned}\tag{1.1}$$

Here, t is the time and s the parameter determining a material cross section of the rod. The unit-quaternions \mathbf{q} and the associated orthogonal matrix $D(\mathbf{q})$ describe the transformation between the fixed external basis and the director-basis. The vector fields \mathbf{v} , \mathbf{u} , \mathbf{p} , and \mathbf{w} are the tangent of the curve, the generalized curvature, the velocity, and the angular velocity, respectively. Moreover, (ρA) is the rod's line density and the positive definite matrix (ρJ) is defined by the moments of inertia of its cross sections. In this paper the contact force \mathbf{n} and the contact couple \mathbf{m} are specified by a hyperelastic material law. In Section 3 we introduce the concept of energy as a constant of motion. In Section 4 we develop a straightforward finite difference scheme for the above equations with appropriate boundary conditions. The scheme conserves the energy and the orthonormality of the directors. In Section 5 the method is investigated for several examples using Timoshenko's material law.

2. Model

Following Antman [10], a special Cosserat rod in the three-dimensional Euclidian space \mathbb{E}^3 is geometrically characterized by three vector-valued functions $\mathbf{r}, \mathbf{d}_1, \mathbf{d}_2 : (s_a, s_b) \times \mathbb{R} \rightarrow \mathbb{E}^3$. The parameter $s \in (s_a, s_b) \subset \mathbb{R}$ identifies a material cross section (material point) of the rod, $\mathbf{r}(s, t)$ characterizes the position of this cross section at time t . The derivatives of the curve \mathbf{r} with respect to t and s ,

$$\mathbf{p} = \partial_t \mathbf{r}, \quad \mathbf{v} = \partial_s \mathbf{r},\tag{2.1}$$

are the velocity and the tangent field. The orthonormal directors $\mathbf{d}_1, \mathbf{d}_2$ characterize the orientation of the cross sections. Defining $\mathbf{d}_3 = \mathbf{d}_1 \times \mathbf{d}_2$, we get a local orthonormal basis at all material points. Due to the orthonormality of the directors there exist vector-valued functions \mathbf{u} and \mathbf{w} such that

$$\partial_t \mathbf{d}_k = \mathbf{w} \times \mathbf{d}_k, \quad \partial_s \mathbf{d}_k = \mathbf{u} \times \mathbf{d}_k\tag{2.2}$$

for $k \in \{1, 2, 3\}$. We call \mathbf{w} the angular velocity and \mathbf{u} the generalized curvature. The definitions of the vector fields \mathbf{p} , \mathbf{v} , \mathbf{w} , and \mathbf{u} imply the compatibility conditions:

$$\partial_t \mathbf{v} = \partial_s \mathbf{p}, \quad \partial_t \mathbf{u} = \partial_s \mathbf{w} + \mathbf{w} \times \mathbf{u}, \quad (2.3)$$

that complete the kinematic equations of the the special Cosserat rod theory in an invariant notation.

To rewrite these kinematic equations in an appropriate basis, we decompose an arbitrary vector field \mathbf{x} of our rod theory in the director-basis \mathbf{d}_k as well as in a fixed external Cartesian basis \mathbf{e}_k , that is, $\mathbf{x} = \sum_{k=1}^3 x_k \mathbf{d}_k = \sum_{k=1}^3 \bar{x}_k \mathbf{e}_k \in \mathbb{E}^3$. The corresponding component triple,

$$\mathbf{x} = (x_1, x_2, x_3) \in \mathbb{R}^3, \quad \bar{\mathbf{x}} = (\bar{x}_1, \bar{x}_2, \bar{x}_3) \in \mathbb{R}^3, \quad (2.4)$$

are strictly to distinguish from the vector field $\mathbf{x} \in \mathbb{E}^3$. The component triples of its derivatives with respect to t and s in the director-basis are

$$(\partial_t \mathbf{x} \cdot \mathbf{d}_k)_{k=1,2,3} = \partial_t \mathbf{x} + \mathbf{w} \times \mathbf{x}, \quad (\partial_s \mathbf{x} \cdot \mathbf{d}_k)_{k=1,2,3} = \partial_s \mathbf{x} + \mathbf{u} \times \mathbf{x}. \quad (2.5)$$

The transformation between the director-basis and the external basis is given by an orthonormal matrix D with components $D_{ij} = \mathbf{d}_i \cdot \mathbf{e}_j$. We use a representation of D in unit-quaternions $\mathbf{q} = (q_0, q_1, q_2, q_3) \in \mathbb{R}^4$, cf. [16],

$$D = D(\mathbf{q}) = \begin{pmatrix} q_0^2 + q_1^2 - q_2^2 - q_3^2 & 2(q_1 q_2 - q_0 q_3) & 2(q_1 q_3 + q_0 q_2) \\ 2(q_1 q_2 + q_0 q_3) & q_0^2 - q_1^2 + q_2^2 - q_3^2 & 2(q_2 q_3 - q_0 q_1) \\ 2(q_1 q_3 - q_0 q_2) & 2(q_2 q_3 + q_0 q_1) & q_0^2 - q_1^2 - q_2^2 + q_3^2 \end{pmatrix}. \quad (2.6)$$

Here, the orthonormality of the matrix $D(\mathbf{q})$ is guaranteed by $\|\mathbf{q}\| = 1$. For an arbitrary $\mathbf{x} \in \mathbb{E}^3$ with $\mathbf{x} = \sum_{k=1}^3 x_k \mathbf{d}_k = \sum_{k=1}^3 \bar{x}_k \mathbf{e}_k$ we obtain $\mathbf{x} = D(\mathbf{q}) \cdot \bar{\mathbf{x}}$. Instead of the kinematic equation for the directors, we formulate an equivalent equation for the quaternions, cf. [16],

$$\partial_t \mathbf{q} = \frac{1}{2} \begin{pmatrix} 0 & w_1 & w_2 & w_3 \\ -w_1 & 0 & -w_3 & w_2 \\ w_2 & w_3 & 0 & -w_1 \\ -w_3 & w_2 & w_1 & 0 \end{pmatrix} \cdot \mathbf{q} = \mathbf{\Omega}(w) \cdot \mathbf{q}. \quad (2.7)$$

Initializing (2.7) with the unit-quaternions, the skew symmetry of $\mathbf{\Omega}(w)$ guarantees the preservation of the norm of the quaternions in time, that is, the orthonormality of $D(\mathbf{q})$ and hence

the orthonormality of the director-basis. Using the presented formalism we obtain our final version of the kinematic equations of the rod:

$$\begin{aligned}\partial_t \bar{\mathbf{r}} &= D(\mathbf{q})^{-1} \cdot \mathbf{p}, \\ \partial_t \mathbf{q} &= \boldsymbol{\Omega}(\mathbf{w}) \cdot \mathbf{q}, \\ \partial_t \mathbf{v} &= \partial_s \mathbf{p} + \mathbf{u} \times \mathbf{p} + \mathbf{v} \times \mathbf{w}, \\ \partial_t \mathbf{u} &= \partial_s \mathbf{w} + \mathbf{u} \times \mathbf{w}.\end{aligned}\tag{2.8}$$

The balance laws for momentum and angular momentum yield the dynamic equations of the Cosserat rod theory, cf. [10],

$$\begin{aligned}(\rho A) \partial_t \mathbf{p} &= \partial_s \mathbf{n} + \mathbf{f}, \\ \sum_{\alpha, \beta=1,2} (\rho J^{\alpha\beta}) \partial_t (\mathbf{d}_\alpha \times \partial_t \mathbf{d}_\beta) &= \partial_s \mathbf{m} + \mathbf{v} \times \mathbf{n} + \mathbf{l}.\end{aligned}\tag{2.9}$$

Here, (ρA) is the line-density and $(\rho J^{\alpha\beta})$ are the moments of inertia. These quantities are time independent, since they are defined in the reference configuration as Lagrangian quantities. We assume that they are constant with respect to s , too. The body force line density \mathbf{f} has to be specified in the applications. We assume $\mathbf{l} = \mathbf{0}$ for the corresponding body couple density. The contact force \mathbf{n} and contact couple \mathbf{m} have to be defined by material laws. Usually, this is done in the director-basis for reasons of objectivity. Thus, we decompose also the dynamical equations in the director-basis:

$$\begin{aligned}\partial_t \mathbf{p} &= \frac{1}{(\rho A)} \partial_s \mathbf{n} + \frac{1}{(\rho A)} \mathbf{u} \times \mathbf{n} + \mathbf{p} \times \mathbf{w} + \frac{1}{(\rho A)} D \cdot \bar{\mathbf{f}}, \\ \partial_t \mathbf{w} &= (\rho J)^{-1} \cdot \partial_s \mathbf{m} + (\rho J)^{-1} \cdot (\mathbf{u} \times \mathbf{m} + \mathbf{v} \times \mathbf{n} + ((\rho J) \cdot \mathbf{w}) \times \mathbf{w}).\end{aligned}\tag{2.10}$$

The positive definite matrix (ρJ) is given by the moments of inertia:

$$(\rho J) = \begin{pmatrix} (\rho J^{22}) & -(\rho J^{12}) & 0 \\ -(\rho J^{21}) & (\rho J^{11}) & 0 \\ 0 & 0 & (\rho J^{11}) + (\rho J^{22}) \end{pmatrix}.\tag{2.11}$$

The body force, for example, gravity, is obviously defined in the external basis. Thus, (2.10) are coupled to the kinematic equation for the quaternions.

Remark 2.1. The special Cosserat rod theory describes the angular momentum as a linear function of the angular velocity. The choice of the representation of the vector fields in the director-basis leads to the time independent matrix (ρJ) characterizing this linear dependence. Besides the proper formulation of the material laws, this time independence is one of the major advantages of the choice of the director-basis.

In this paper we restrict ourselves to hyperelastic materials. That means there exists a potential $\mathbb{R}^6 \ni (v, u) \mapsto \psi(v, u) \in \mathbb{R}$, such that

$$n = \partial_v \psi, \quad m = \partial_u \psi. \quad (2.12)$$

Moreover, we assume that only potential forces act on the rod. Thus there exists a function $\mathbb{R}^3 \ni \bar{r} \mapsto V(\bar{r}) \in \mathbb{R}$, such that

$$\bar{f} = -\partial_{\bar{r}} V. \quad (2.13)$$

Remark 2.2. The more general class of elastic materials are materials where n and m are functions of the so-called strain variables v and u . These functions may also depend explicitly on s .

The kinematic equations (2.8) and the dynamic equations (2.10) together with the restriction to hyperelastic materials and potential forces constitute our rod theory, see also (1.1). We consider system (1.1) with two types of boundary conditions defining a fixed or a free end. For simplicity we restrict our description to a fixed end at $s = s_a$

$$p(s_a, t) = 0, \quad w(s_a, t) = 0, \quad (2.14)$$

and a free end at $s = s_b$

$$n(s_b, t) = 0, \quad m(s_b, t) = 0. \quad (2.15)$$

The presentation of the energy conserving numerical algorithm in Section 4 deals with the above general class of rods. For the numerical examples in Section 5 we specify the rod's geometry, a hyperelastic material law, and the potential forces. We consider a homogeneous cylinder with diameter $d > 0$, cross section area $A = \pi/4d^2$, and moment of inertia $I = \pi/64d^4$. In this case, the matrix of inertia is

$$(\rho J) = (\rho I) \text{diag}(1, 1, 2). \quad (2.16)$$

We use the material law of Timoshenko [17] for Poisson number $\mu = 1/2$:

$$\psi = \frac{1}{2}(EA) \left(\frac{1}{3}v_1^2 + \frac{1}{3}v_2^2 + (v_3 - 1)^2 \right) + \frac{1}{2}(EI) \left(u_1^2 + u_2^2 + \frac{2}{3}u_3^2 \right), \quad (2.17)$$

where E is Young's modulus. Additionally, we restrict to gravitational forces, that is,

$$V = -(\rho A) g e_g \cdot \bar{r}, \quad (2.18)$$

where g is the gravitational constant and e_g is the direction of gravity in the external Cartesian basis.

Remark 2.3. For hyperelastic materials (1.1) is an inhomogeneous hyperbolic system. In the special case of Timoshenko for a homogeneous cylinder the hyperbolic part is linear with eigenvalues 0 (sevenfold), $\pm c$ (threefold), and $\pm c/3$ (threefold), where $c = \sqrt{E/\rho}$ is the speed of sound. Computing the eigenvectors one can easily show that the fixed and free end boundary condition correctly handle the characteristic variables \bar{r} and q corresponding to the eigenvalue 0. With respect to the remaining variables we do not prescribe characteristic variables, but the correct number of variables on both sides of the rod.

3. Energy as a Constant of Motion

The system (1.1) for the state vector $\boldsymbol{\phi} = (\bar{r}, q, v, u, p, w) \in \mathbb{R}^{19}$ can be written in the general form of a conservation law as

$$\partial_t \boldsymbol{\phi} = \partial_s \mathbf{f}(\boldsymbol{\phi}) + \mathbf{h}(\boldsymbol{\phi}) \quad (3.1)$$

with flux-function $\mathbf{f}(\boldsymbol{\phi}) = (0, 0, p, w, (1/(\rho A))n, (\rho J)^{-1} \cdot m)$ and source term $\mathbf{h}(\boldsymbol{\phi})$ that is easy to identify from (1.1). We introduce the energy density:

$$\varepsilon(\boldsymbol{\phi}) = \frac{1}{2}(\rho A)p^2 + \frac{1}{2}w \cdot (\rho J) \cdot w + \psi(v, u) + V(\bar{r}). \quad (3.2)$$

and the symmetric function:

$$a(\boldsymbol{\phi}_1, \boldsymbol{\phi}_2) = \frac{1}{2}(n_1 \cdot p_2 + m_1 \cdot w_2 + p_1 \cdot n_2 + w_1 \cdot m_2) \quad (3.3)$$

for arbitrary states $\boldsymbol{\phi}_1, \boldsymbol{\phi}_2$. The derivative of the energy density with respect to the state vector $\boldsymbol{\phi}$ is given by

$$\partial_{\boldsymbol{\phi}} \varepsilon = (-\bar{f}, 0, n, m, (\rho A)p, (\rho J) \cdot w), \quad (3.4)$$

that leads to the properties:

$$\partial_{\boldsymbol{\phi}} \varepsilon \cdot \mathbf{h} = 0, \quad \frac{1}{2} \partial_{\boldsymbol{\phi}} \varepsilon(\boldsymbol{\phi}_1) \cdot \mathbf{f}(\boldsymbol{\phi}_2) = a(\boldsymbol{\phi}_1, \boldsymbol{\phi}_2), \quad \partial_{\boldsymbol{\phi}} \varepsilon \cdot \partial_s \mathbf{f} = \partial_s a(\boldsymbol{\phi}, \boldsymbol{\phi}). \quad (3.5)$$

We conclude the local energy balance:

$$\partial_t \varepsilon = \partial_s a(\boldsymbol{\phi}, \boldsymbol{\phi}), \quad (3.6)$$

that is, $a(\boldsymbol{\phi}, \boldsymbol{\phi})$ is the energy flux and there is no energy source term. For the presented fixed and free end boundary conditions (2.14), (2.15) we have a vanishing energy flux at the boundaries. Therefore, the total energy is a constant of motion:

$$\frac{d}{dt} \mathcal{E} = \frac{d}{dt} \int_{s_a}^{s_b} \varepsilon ds' = 0. \quad (3.7)$$

4. Discretization

For the spatial discretization we use a simple finite difference scheme. We note that similar finite difference schemes have been developed and their properties, in particular, the conservation of invariants, have been investigated in [8, 12, 18].

We discretize (s_a, s_b) with $(N + 1)$ equidistant mesh points s_j and denote the corresponding length of the cells by Δs . The boundary points are $s_1 = s_a$ and $s_{N+1} = s_b$. As usual, the numerical fluxes are denoted by $\mathbf{F}_{j+1/2}$ for all $j \in \{1, \dots, N\}$. The state vector and the source terms are discretely given at the mesh points $j \in \{1, \dots, N+1\}$, that is, $\boldsymbol{\phi}_j \simeq \boldsymbol{\phi}(s_j, t)$ and $\mathbf{H}_j \simeq \mathbf{h}(\boldsymbol{\phi}(s_j, t))$. For the inner points $j \in \{2, \dots, N\}$ the spatial discretization results in

$$\frac{d}{dt} \boldsymbol{\phi}_j = \frac{1}{\Delta s} [\mathbf{F}_{j+1/2} - \mathbf{F}_{j-1/2}] + \mathbf{H}_j, \quad \mathbf{F}_{j+1/2} \simeq \frac{1}{2} [\mathbf{f}(\boldsymbol{\phi}_j) + \mathbf{f}(\boldsymbol{\phi}_{j+1})]. \quad (4.1)$$

Thereby, the numerical flux function is approximated by the arithmetic average of the flux at neighboring mesh points. For the flux calculation at the boundaries we have to fulfill the Dirichlet boundary conditions at the fixed end $s_a = s_1$:

$$p_1 = 0, \quad w_1 = 0, \quad (4.2)$$

and at the free end $s_b = s_{N+1}$:

$$n_{N+1} = 0, \quad m_{N+1} = 0. \quad (4.3)$$

Thus, for the remaining components our finite difference scheme reads at the fixed end $s_a = s_1$:

$$\frac{d}{dt} \bar{r}_1 = 0, \quad \frac{d}{dt} q_1 = 0, \quad \frac{d}{dt} v_1 = \frac{1}{\Delta s} p_2, \quad \frac{d}{dt} u_1 = \frac{1}{\Delta s} w_2, \quad (4.4)$$

and at the free end $s_b = s_{N+1}$:

$$\begin{aligned} \frac{d}{dt} \bar{r}_{N+1} &= \mathbf{D}^{-1}(\mathbf{q}_{N+1}) \cdot \mathbf{p}_{N+1}, & \frac{d}{dt} \mathbf{q}_{N+1} &= \boldsymbol{\Omega}(\mathbf{w}_{N+1}) \cdot \mathbf{q}_{N+1}, \\ \frac{d}{dt} \mathbf{p}_{N+1} &= -\frac{1}{\Delta s} \frac{1}{\rho A} \mathbf{n}_N + \mathbf{p}_{N+1} \times \mathbf{w}_{N+1} + \frac{1}{(\rho A)} \mathbf{D}(\mathbf{q}_{N+1}) \cdot \bar{\mathbf{f}}_{N+1}, & (4.5) \\ \frac{d}{dt} \mathbf{w}_{N+1} &= -\frac{1}{\Delta s} (\rho \mathbf{J})^{-1} \cdot \mathbf{m}_N + (\rho \mathbf{J})^{-1} \cdot ((\rho \mathbf{J}) \cdot \mathbf{w}_{N+1}) \times \mathbf{w}_{N+1}. \end{aligned}$$

Now, we come up with our main point, the (semi)discrete energy conservation of this scheme. The energy density is approximated locally at the mesh points $j \in \{1, \dots, N+1\}$, that is, $\varepsilon_j \simeq \varepsilon(\boldsymbol{\phi}_j)$. We obtain for the inner points $j \in \{2, \dots, N\}$:

$$\begin{aligned} \frac{d}{dt} \varepsilon_j &= \partial_{\boldsymbol{\phi}} \varepsilon(\boldsymbol{\phi}_j) \cdot \frac{d}{dt} \boldsymbol{\phi}_j \stackrel{(19)}{=} \partial_{\boldsymbol{\phi}} \varepsilon(\boldsymbol{\phi}_j) \cdot \left[\frac{1}{\Delta s} (\mathbf{F}_{j+1/2} - \mathbf{F}_{j-1/2}) + \mathbf{H}_j \right] \\ &\stackrel{(17)}{=} \frac{1}{\Delta s} \left[a(\boldsymbol{\phi}_j, \boldsymbol{\phi}_{j+1}) - a(\boldsymbol{\phi}_{j-1}, \boldsymbol{\phi}_j) \right]. \end{aligned} \quad (4.6)$$

For the boundaries we have to take into account the Dirichlet conditions:

$$\begin{aligned} \frac{d}{dt} \varepsilon_1 &= \partial_{\boldsymbol{\phi}} \varepsilon(\boldsymbol{\phi}_1) \cdot \frac{d}{dt} \boldsymbol{\phi}_1 \stackrel{(16,20,22)}{=} \frac{1}{\Delta s} (\mathbf{n}_1 \cdot \mathbf{p}_2 + \mathbf{m}_1 \cdot \mathbf{w}_2) \\ &\stackrel{(15,20)}{=} \frac{2}{\Delta s} a(\boldsymbol{\phi}_1, \boldsymbol{\phi}_2), \\ \frac{d}{dt} \varepsilon_{N+1} &= \partial_{\boldsymbol{\phi}} \varepsilon(\boldsymbol{\phi}_{N+1}) \cdot \frac{d}{dt} \boldsymbol{\phi}_{N+1} \stackrel{(16,20,23)}{=} -\frac{1}{\Delta s} (\mathbf{n}_N \cdot \mathbf{p}_{N+1} + \mathbf{m}_N \cdot \mathbf{w}_{N+1}) \\ &\stackrel{(15,21)}{=} -\frac{2}{\Delta s} a(\boldsymbol{\phi}_N, \boldsymbol{\phi}_{N+1}). \end{aligned} \quad (4.7)$$

Applying the trapezoidal quadrature rule for the discrete energy,

$$\boldsymbol{\varepsilon} \simeq \boldsymbol{\varepsilon}^{\text{Disc}} = \frac{\Delta s}{2} \varepsilon_1 + \Delta s \sum_{j=2}^N \varepsilon_j + \frac{\Delta s}{2} \varepsilon_{N+1}, \quad (4.8)$$

guarantees its conservation:

$$\frac{d}{dt} \boldsymbol{\varepsilon}^{\text{disc}} = \frac{\Delta s}{2} \frac{d}{dt} \varepsilon_1 + \Delta s \sum_{j=2}^N \frac{d}{dt} \varepsilon_j + \frac{\Delta s}{2} \frac{d}{dt} \varepsilon_{N+1} = 0. \quad (4.9)$$

This means, the chosen semidiscretization in space ensures that the discrete energy (4.8) is a first integral of the ODE-system (4.1)–(4.5).

For the time discretization any energy conserving method can be used. We choose a Gauss method, that also guarantees the preservation of the norm of the quaternions. In the numerical realization, we make use of the second order Gauss method, that is, the midpoint rule, to obtain a temporal order that is consistent with the spatial one, at least at the inner points. For the discretization of space and time, and the use of the midpoint rule for the conservation of certain properties we refer also to the above mentioned papers [12, 18].

To solve the resulting nonlinear equations a Newton method is used. The strict conservation of energy and orthogonality are the main advantages of the straightforward finite difference scheme presented here.

Remark 4.1. The scheme described above concentrates on preserving the energy of the rod and the orthonormality of the directors. In the sense of numerical methods for hyperbolic systems the scheme is not able to handle shocks properly. It does not have the usual properties like being a TVD scheme or satisfying the entropy condition.

Remark 4.2. Higher order discretizations are also possible. For example, we could consider the following fourth order numerical flux function:

$$F_{j+1/2} \approx \frac{1}{2} [f(\phi_j) + f(\phi_{j+1})] + \frac{1}{16} [-f(\phi_{j+2}) + f(\phi_{j+1}) + f(\phi_j) - f(\phi_{j-1})]. \tag{4.10}$$

Then, the time derivative of the discrete energy density at the inner mesh point j is given by

$$\frac{d}{dt} \varepsilon_j = \frac{1}{\Delta s} \left[\underbrace{a(\phi_j, \phi_{j+1})}_{=O_1} - \underbrace{a(\phi_{j-1}, \phi_j)}_{=U_1} \right. \\ \left. \underbrace{-\frac{1}{8} a(\phi_j, \phi_{j+2})}_{=O_3} + \underbrace{\frac{1}{4} a(\phi_j, \phi_{j+1})}_{=O_2} - \underbrace{\frac{1}{4} a(\phi_{j-1}, \phi_j)}_{=U_2} + \underbrace{\frac{1}{8} a(\phi_{j-2}, \phi_j)}_{=U_3} \right]. \tag{4.11}$$

The terms $O_1, O_2, O_3, U_1, U_2,$ and U_3 are eliminated at the mesh points $j+1, j+1, j+2, j-1, j-1,$ and $j-2,$ respectively. Neglecting the boundary points this yields again the conservation of the discrete energy. The discretization near the boundary points has to be considered separately.

5. Numerical Examples

In this section we present three numerical examples, restricting ourselves to Timoshenko’s material law for a homogeneous cylinder as discussed at the end of Section 2. Introducing a typical length, a typical time, and a typical mass:

$$s_{\text{typ}} = s_b - s_a, \quad t_{\text{typ}} = \frac{s_{\text{typ}}}{\sqrt{E/\rho}}, \quad m_{\text{typ}} = \rho \frac{\pi}{4} d^2 s_{\text{typ}}, \tag{5.1}$$

the dimensionless parameters of the model are the slenderness ratio and the gravity number:

$$\delta = \frac{d}{s_{\text{typ}}}, \quad \gamma = \frac{\rho g s_{\text{typ}}}{E}. \tag{5.2}$$

In more details, we have $(EA) = (\rho A) = 1, (EI) = (\rho I) = \pi/16\delta^2,$ and for the speed of sound $c = 1.$ In the dimensionless form Timoshenko’s material law reads

$$n = \left(\frac{1}{3} v_1, \frac{1}{3} v_2, v_3 - 1 \right), \quad m = \frac{\pi}{16} \delta^2 \left(u_1, u_2, \frac{2}{3} u_3 \right). \tag{5.3}$$

To simplify the formulation of the equations we define for $x \in \mathbb{R}^3$ and $\lambda \in \mathbb{R}$:

$$[x]_\lambda = (x_1, x_2, \lambda x_3), \quad \hat{x} = (-x_2, x_1, 0). \quad (5.4)$$

Then, the system (1.1) reads

$$\begin{aligned} \partial_t \bar{r} &= D^{-1}(q) \cdot p, \\ \partial_t q &= \Omega(w) \cdot q, \\ \partial_t v &= \partial_s p + u \times p + v \times w, \\ \partial_t u &= \partial_s w + u \times w, \\ \partial_t p &= \frac{1}{3} \partial_s [v]_3 + \frac{1}{3} u \times [v]_3 + \hat{u} + p \times w - \gamma D(q) \cdot (0, 1, 0), \\ \partial_t w &= \partial_s [u]_{1/3} + \frac{1}{3} u_3 \hat{u} + \frac{16}{\pi} \frac{1}{\delta^2} \left(1 - \frac{2}{3} v_3 \right) \hat{v} + w_3 \hat{w}. \end{aligned} \quad (5.5)$$

As mentioned, the rod is fixed at one side,

$$p(0, t) = (0, 0, 0), \quad w(0, t) = (0, 0, 0), \quad (5.6)$$

and the other side is free, that is, for Timoshenko's material law:

$$v(1, t) = (0, 0, 1), \quad u(1, t) = (0, 0, 0). \quad (5.7)$$

The chosen initial configuration of a straight rod and direction of gravity $e_g = (0, -1, 0)$ can be seen in Figure 1. In the following examples different initial torsions will be considered. More precisely,

$$\begin{aligned} r(s, 0) &= s d_3, \\ d_1(s, 0) &= e_2 \cos(\mu(s)) + e_3 \sin(\mu(s)), \\ d_2(s, 0) &= -e_2 \sin(\mu(s)) + e_3 \cos(\mu(s)), \end{aligned} \quad (5.8)$$

where $\mu : (0, 1) \rightarrow \mathbb{R}$ is a field of torsion angles that has to be defined. These conditions are equivalent to initial conditions for $\bar{r}(s, 0)$ and $q(s, 0)$. Moreover, due to the definitions of v and u we have

$$v(s, 0) = (0, 0, 1), \quad u(s, 0) = (0, 0, \partial_s \mu). \quad (5.9)$$

Finally we prescribe

$$p(s, 0) = (0, 0, 0), \quad w(s, 0) = (0, 0, 0), \quad (5.10)$$

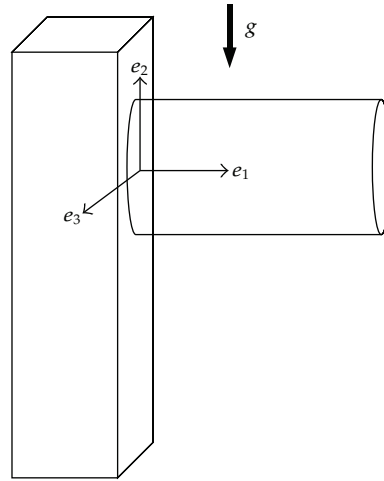


Figure 1: Initial situation.

that is, the rod is initially at rest. Our initial conditions are compatible to the boundary conditions if $\mu(0) = 0$ and $\partial_s \mu(1) = 0$.

In all simulations we choose the CFL-number equal to 1. This implies $\Delta t = \Delta s$ as for the speed of sound $c = 1$ in the dimensionless form.

We remark that in all simulations energy is strictly conserved according to the above analysis.

Example 5.1 (Torsional Oscillation without Gravity). We choose $\gamma = 0$, $\delta = 10^{-3}$, and a field of torsion angles fulfilling the compatibility condition:

$$\mu(s) = \frac{2}{\pi} \sin\left(\frac{\pi}{2}s\right). \quad (5.11)$$

In this example, only the torsion u_3 and the angular velocity w_3 are involved, because of the vanishing gravity. The equations reduce to the homogenous wave-equation:

$$\begin{aligned} \partial_t u_3 - \partial_s w_3 &= 0, \\ \partial_t w_3 - \frac{1}{3} \partial_s u_3 &= 0. \end{aligned} \quad (5.12)$$

Due to the chosen torsion angle we exactly initialize the fundamental mode of the wave equation with a frequency

$$\omega_{\text{theo}} = \frac{\pi}{\sqrt{12}}. \quad (5.13)$$

We use this example as a benchmark for the convergence properties of our scheme comparing the computed frequencies with the analytical one for different grid sizes, see Figure 2. Comparing the identified simulation frequency with the fundamental frequency of the analytical

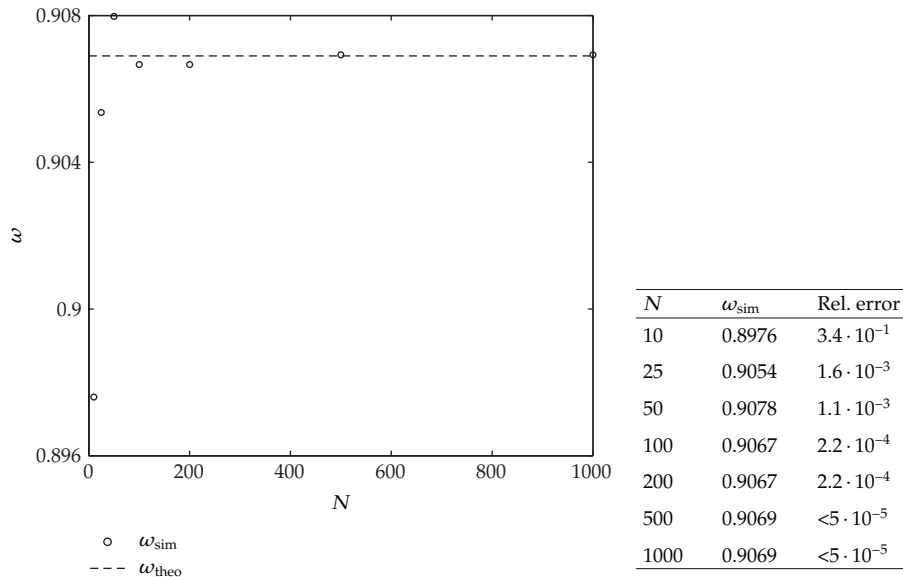


Figure 2: Torsional oscillation-Frequency ω versus number of grid cells N .

solution $\omega_{\text{theo}} = 0.9069$ we note that, for example, for $N = 25$ the relative error is of the order 10^{-3} .

Example 5.2 (Transversal Oscillation). We choose $\gamma = 10^{-7}$, $\mu = 0$, and vary δ from 10^{-3} to 10^{-1} . This example describes the classical case of transversal oscillation of an one-sided fixed rod without twist. Since the rod is strainless in the initial configuration and—as mentioned—at rest initially, gravity is used to excite the oscillation. The transversal oscillation frequency for the rod can be compared to the well-known result for vanishing gravitation given for example in Peterson [19] or Timoshenko [20]. It reads in the chosen dimensionless form

$$\omega = \frac{\lambda^2}{4} \delta, \quad (5.14)$$

where the constant λ is given by $\lambda = 1,875$. Defining the temporal difference between two maxima of the potential energy as a period of oscillation, we identify the frequency ω_{sim} . Figure 3 shows for $N = 10$ the expected linearity of the frequency ω with respect to the slenderness ratio δ . Determining λ from a best fit line, we obtain $\lambda_{\text{sim}} = 1.870$. Thus, the relative error is very small—of the order 10^{-3} —even for the very coarse discretization with $N = 10$.

We note that the solution is very accurate although we have chosen a linear material law for the contact force \mathbf{n} instead of a Kirchhoff constraint $\mathbf{v} = (0, 0, 1)$ normally used.

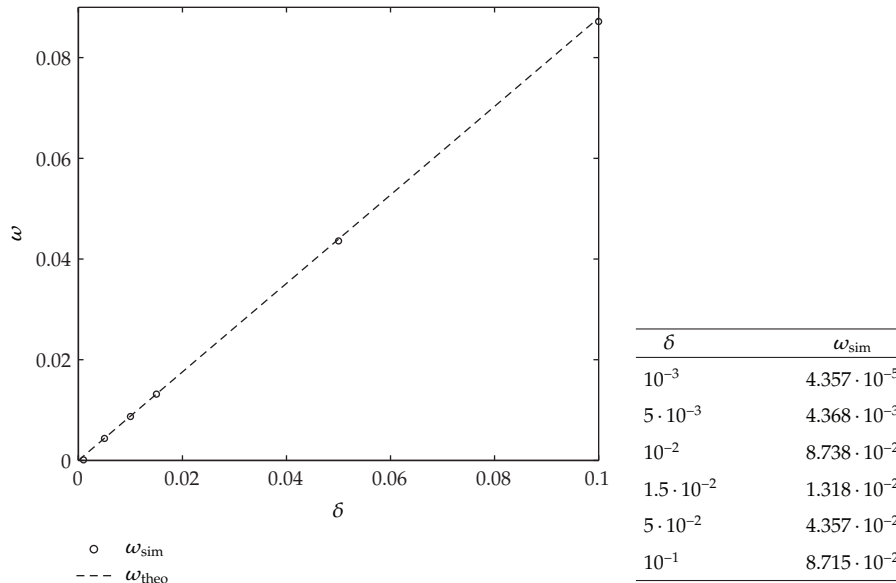


Figure 3: Transversal oscillation-frequency ω versus slenderness δ .

Example 5.3 (Three-dimensional Problem Including all Strain Variables). We choose $\gamma = 10^{-4}$, $\delta = 10^{-2}$, and a field of torsion angles:

$$\mu = 6\pi s(2 - s). \tag{5.15}$$

In this case, see Figure 4, the rod is initially twisted three times and the gravitational number is comparatively high. That means all strain variables of the rod are excited during the evolution. The algorithm is able to deal with such a situation, in particular, from the point of view of conservation of energy. The results are reasonable as long as the linear material law is valid. One has to take into account that for large strain values Timoshenko’s material law does not guarantee that the deformation of the rod preserves the orientation. See Antman [10] for a precise definition of the preservation of orientation.

6. Conclusion

In this paper we use the description of a hyperelastic rod in the formulation of Antman [10]. For the resulting hyperbolic system we developed a numerical method, which conserves the energy of the rod as well as the orthonormality of the directors. However, the scheme is not able to handle shocks properly. It is neither a TVD scheme nor does it satisfy the entropy condition.

For the material law of Timoshenko [17] we illustrated the method using some numerical examples. For these examples, the conservation properties are strictly fulfilled and very good agreement of the numerical and analytical results can be observed. Finally, we mention that for realistic three-dimensional problems a nonlinear material law has to be used, which can be easily incorporated in the scheme.

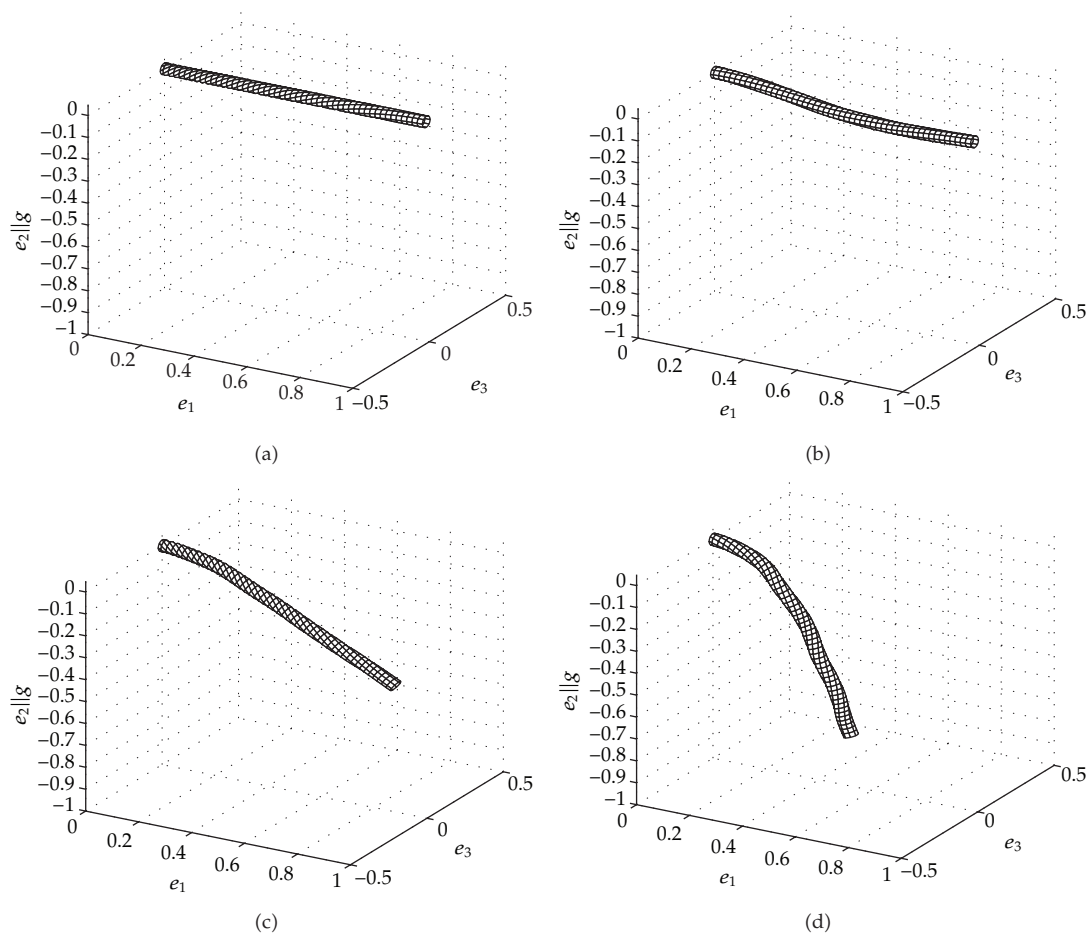


Figure 4: Rod's curve at $t = 0$ (a), $t = 40$ (b), $t = 80$ (c), and $t = 120$ (d).

Acknowledgments

This work has been supported by Deutsche Forschungsgemeinschaft (DFG), KL 1105/18-1 and WE 2003/3-1 and by Rheinland-Pfalz Excellence Center for Mathematical and Computational Modeling (CM)².

References

- [1] D. K. Pai, "Interactive simulation of thin solids using Cosserat models," *Computer Graphics Forum*, vol. 21, no. 3, pp. 347–352, 2002.
- [2] J. Barbic and D. James, "Real-time subspace integration for St. Venant-Kirchhoff deformable models," *ACM Transactions on Graphics*, vol. 24, no. 3, pp. 982–990, 2005.
- [3] A. Weber, T. Lay, and G. Sobottka, "Stable integration of the dynamic Cosserat equations with application to hair modeling," *Journal of WSCG*, vol. 16, pp. 73–80, 2008.
- [4] J. C. Simo, "A finite beam formulation. The three dimensional dynamic problem. Part I," *Computer Methods in Applied Mechanics and Engineering*, vol. 49, pp. 55–70, 1985.
- [5] J. C. Simo and L. Vu-Quoc, "A three dimensional finite-strain rod model. Part II: computational aspects," *Computer Methods in Applied Mechanics and Engineering*, vol. 58, pp. 79–116, 1986.

- [6] J. C. Simo and L. Vu-Quoc, "On the dynamics in space of rods undergoing large motions—a geometrically exact approach," *Computer Methods in Applied Mechanics and Engineering*, vol. 66, no. 2, pp. 125–161, 1988.
- [7] J. C. Simo, J. E. Marsden, and P. S. Krishnaprasad, "The Hamiltonian structure of nonlinear elasticity: the material and convective representations of solids, rods, and plates," *Archive for Rational Mechanics and Analysis*, vol. 104, no. 2, pp. 125–183, 1988.
- [8] L. Vu-Quoc and X. Tan, "Optimal solid shells for nonlinear analyses of multilayer composites. part ii: dynamics," *Computer Methods in Applied Mechanics and Engineering*, vol. 192, no. 9-10, pp. 1017–1059, 2003.
- [9] E. Wittbrodt, I. Adamiec-Wojcik, and S. Wojciech, *Dynamic of Flexible Multibody Systems*, Springer, 2006.
- [10] S. S. Antman, *Nonlinear Problems of Elasticity*, Springer, New York, NY, USA, 2005.
- [11] J. C. Simo, N. Tarnow, and K. K. Wong, "Exact energymomentum conserving algorithms and symplectic schemes for nonlinear dynamics," *Computer Methods in Applied Mechanics and Engineering*, vol. 100, no. 1, pp. 63–116, 1992.
- [12] S. Li and L. Vu-Quoc, "Finite difference calculus invariant structure of a class of algorithms for the nonlinear Klein-Gordon equation," *SIAM Journal on Numerical Analysis*, vol. 32, no. 6, pp. 1839–1875, 1995.
- [13] L. Vu-Quoc and J. Simo, "On the dynamics of earth-orbiting flexible satellites with multibody components," *AIAA Journal of Guidance, Control, and Dynamics*, vol. 10, no. 6, pp. 549–558, 1987.
- [14] L. Vu-Quoc, *Dynamics of flexible structures performing large overall motions: a geometrically-nonlinear approach, technical report no. UCB/ERL M86/36 [Ph.D. thesis]*, University of California at Berkeley, 1986.
- [15] F. A. McRobie and J. Lasenby, "Simo-Vu Quoc rods using Clifford algebra," *International Journal for Numerical Methods in Engineering*, vol. 45, no. 4, pp. 377–398, 1999.
- [16] L. Mahadevan and J. B. Keller, "Coiling of flexible ropes," *Proceedings of the Royal Society A*, vol. 452, no. 1950, pp. 1679–1694, 1996.
- [17] S. P. Timoshenko, "On the correction for shear of differential equations for transverse vibrations of prismatic bars," *Philosophical Magazine*, vol. 6, no. 41, pp. 744–746, 1921.
- [18] L. Vu-Quoc and S. Li, "Invariant-conserving finite difference algorithms for the nonlinear Klein-Gordon equation," *Computer Methods in Applied Mechanics and Engineering*, vol. 107, no. 3, pp. 341–391, 1993.
- [19] C. Peterson, *Dynamik der Baukonstruktionen*, Vieweg, 1996.
- [20] S. P. Timoshenko, *Schwingungsproblem der Technik*, Springer, 1932.



Hindawi

Submit your manuscripts at
<http://www.hindawi.com>

